

# Lipschitz-bounded 1D convolutional neural networks using the Cayley transform and the controllability Gramian

Patricia Pauli<sup>1</sup>, Ruigang Wang<sup>2</sup>, Ian R. Manchester<sup>2</sup> and Frank Allgöwer<sup>1</sup>

**Abstract**— We establish a layer-wise parameterization for 1D convolutional neural networks (CNNs) with built-in end-to-end robustness guarantees. Herein, we use the Lipschitz constant of the input-output mapping characterized by a CNN as a robustness measure. We base our parameterization on the Cayley transform that parameterizes orthogonal matrices and the controllability Gramian for the state space representation of the convolutional layers. The proposed parameterization by design fulfills linear matrix inequalities that are sufficient for Lipschitz continuity of the CNN, which further enables unconstrained training of Lipschitz-bounded 1D CNNs. Finally, we train Lipschitz-bounded 1D CNNs for the classification of heart arrhythmia data and show their improved robustness.

## I. INTRODUCTION

Robustness of neural networks (NNs) has lately been a topic of increasing importance, for which the Lipschitz constant of the NN's input-output mapping has become a common metric [1]. Finding an accurate upper bound on an NN's Lipschitz constant has broadly been tackled, e.g. using relaxations by quadratic constraints [2], [3], average operators [4] and polynomial optimization [5]. In addition, the training of provably Lipschitz-bounded NNs was proposed by including constraints [6], [7] and regularization techniques [8]. While effective, one drawback of these techniques is the computational overhead coming from constraints and projections in the optimization problem [7].

To overcome this, [9], [10], [11] suggest direct parameterizations for equilibrium networks, recurrent equilibrium networks, and feedforward neural networks, respectively, with guaranteed Lipschitz bounds. From a set of unconstrained variables [9], [10], [11] formulate the NNs in such a way that they by design satisfy linear matrix inequalities (LMIs). These LMIs in turn are sufficient conditions for Lipschitz continuity such that, this way, one can parameterize the class of Lipschitz-bounded NNs with a Lipschitz upper bound predefined by the user. The underlying training problem boils down to an unconstrained optimization problem that can be solved using gradient methods. In this work, we take the same approach as in [9], [10], [11] to parameterize Lipschitz-bounded 1D convolutional neural networks (CNNs).

\*This work was funded by Deutsche Forschungsgemeinschaft (DFG, German Research Foundation) under Germany's Excellence Strategy - EXC 2075 - 390740016 and under grant 468094890. The authors thank the International Max Planck Research School for Intelligent Systems (IMPRS-IS) for supporting Patricia Pauli.

<sup>1</sup>Patricia Pauli and Frank Allgöwer are with the Institute for Systems Theory and Automatic Control, University of Stuttgart, 70569 Stuttgart, Germany [patricia.pauli@ist.uni-stuttgart.de](mailto:patricia.pauli@ist.uni-stuttgart.de)

<sup>2</sup> Ruigang Wang and Ian R. Manchester are with the Australian Centre for Robotics and School of Aerospace, Mechanical and Mechatronic Engineering, The University of Sydney, Australia.

CNNs have been tremendously successful in image and audio processing tasks and they are the state of the art in these applications [12], [13], [14]. In this paper, we focus on 1D CNNs as a stepping stone to the more relevant, yet more involved case of 2D CNNs, which is beyond the scope of this paper. However, an extension based on a 2D systems representation [15] is possible and left as future work. CNNs typically consist of convolutions, nonlinear activation functions, pooling layers, and linear layers that are concatenated in a feedforward structure. While numerous methods exist for enforcing Lipschitz continuity and orthogonality in fully connected layers [16], the design of Lipschitz bounded convolutional layers and CNNs is less studied and often restricted to special convolutions [17]. Recently, this has been approached via parameterization of convolutional layers in the Fourier domain, however this requires a computationally expensive inverse that depends on the input size [11], [17]. We instead formulate convolutions in state space independent of the input dimension [3], providing us with a compact and nonrepetitive description thereof. This leads to a simple and structurally very similar parameterization to the one for fully connected layers. Another feature of our approach is that we impose Lipschitz continuity onto the input-output mapping only rather than on the individual layers, like it is done in many other works [18], using that the product of the Lipschitz bounds of the layers yields a Lipschitz bound for the overall NN. On the contrary, our approach imposes more general dissipativity properties onto the individual layers [3], yielding a *layer-wise* parameterization with *end-to-end* robustness guarantees. This leads to reduced conservatism in the compliance of the Lipschitz bound, i.e., higher expressivity for the same Lipschitz bound. In addition our approach accounts for standard pooling layers, which were not addressed in other recent Lipschitz-bounded parameterizations of CNNs [11].

Our main contribution is a direct, scalable, and expressive layer-wise parameterization for Lipschitz-bounded 1D CNNs that makes use of the Cayley transform to parameterize orthogonal matrices. Beside the Cayley transform, a tool that was used for NN parameterization before, we newly propose to utilize the controllability Gramian in the context of parameterizing convolutional layers of Lipschitz-bounded CNNs. In particular, we reformulate parts of the underlying LMI, that enforces dissipativity onto convolutional layers, as a Lyapunov equation whose unique analytical solution is the controllability Gramian. Using our parameterization, we then train Lipschitz-bounded 1D CNNs solving an unconstrained optimization problem.

The remainder of the paper is structured as follows: Section II first introduces 1D CNNs and formally states the training problem. In Section III, we discuss preliminaries, including the state space representation for 1D convolutions and the Lipschitz constant estimation for 1D CNNs. In Section IV, we present the direct parameterization for Lipschitz-bounded 1D CNNs and in Section V, we train Lipschitz-bounded 1D CNNs on the MIT-BIH arrhythmia database [19], a well-known benchmark dataset for 1D CNNs. Finally, in Section VI, we conclude the paper.

**Notation:** By  $\mathbb{D}^n$  ( $\mathbb{D}_+^n$ ) and  $\mathbb{S}^n$  ( $\mathbb{S}_+^n$ ), we denote the set of  $n$ -dimensional (positive definite) diagonal and symmetric matrices, respectively, and by  $\mathbb{N}_+$  the natural numbers without zero.  $\mathcal{I}$  is a set of indices with elements  $i \in \mathbb{N}_+$ , and  $|\mathcal{I}|$  gives the number of elements in the index set  $\mathcal{I}$ .

## II. PROBLEM STATEMENT

We consider 1D CNNs that are a concatenation of convolutional layers  $\mathcal{C}_i: \mathbb{R}^{c_{i-1} \times N_{i-1}} \rightarrow \mathbb{R}^{c_i \times N_i}$  with indices  $i \in \mathcal{I}_C$ , and fully connected layers  $\mathcal{L}_i: \mathbb{R}^{n_{i-1}} \rightarrow \mathbb{R}^{n_i}$  with indices  $i \in \mathcal{I}_F$

$$\text{CNN}_\theta = \mathcal{L}_l \circ \dots \circ \mathcal{L}_{p+1} \circ F \circ \mathcal{C}_p \circ \dots \circ \mathcal{C}_1, \quad (1)$$

adding up to a total number of  $l = |\mathcal{I}_C| + |\mathcal{I}_F|$  layers. Herein,  $N_i$  denotes the signal length,  $c_i$  the channel size, and  $n_i$  the layer dimension of the respective  $i$ -th layer. At the intersection of the fully connected part and the fully convolutional part of the CNN, there is a flattening operation  $F: \mathbb{R}^{c_p \times N_p} \rightarrow \mathbb{R}^{n_p}$  of the output of the  $p$ -th (last) convolutional layer with  $n_p = c_p N_p$ .

A *convolutional* layer consists of two to three stages, a convolution operation, a nonlinear activation, and possibly a pooling operation. The first two stages are

$$\tilde{\mathcal{C}}_i: w_k^i = \phi_i \left( b_i + \sum_{j=0}^{\ell_i-1} K_j^i w_{k-j}^{i-1} \right), \quad k = 0, \dots, N_i - 1 \quad \forall i \in \mathcal{I}_C, \quad (2)$$

with convolution kernel  $K_j^i \in \mathbb{R}^{c_i \times c_{i-1}}$ ,  $j = 0, \dots, \ell_i - 1$ , kernel size  $\ell_i$ , and bias  $b_i \in \mathbb{R}^{c_i}$ . First, a convolution on the signal  $w^{i-1} \in \mathbb{R}^{c_{i-1} \times N_{i-1}}$  is applied and subsequently, the nonlinear activation function  $\phi_i: \mathbb{R}^{c_i} \rightarrow \mathbb{R}^{c_i}$  is evaluated elementwise to obtain the output  $w^i \in \mathbb{R}^{c_i \times N_{i-1}}$ . Oftentimes, a convolutional layer additionally contains pooling layers  $\mathcal{P}_i: \mathbb{R}^{c_i \times N_{i-1}} \rightarrow \mathbb{R}^{c_i \times N_i}$  to downsample the signal  $w^i$ . We consider maximum pooling

$$\mathcal{P}_i^{\max}: \tilde{w}_k^i = \max_{j=1, \dots, \ell_i} w_{\ell_i(k-1)+j}^i, \quad k = 0, \dots, N_i - 1, \quad \forall i \in \mathcal{I}_P^{\max},$$

and average pooling

$$\mathcal{P}_i^{\text{av}}: \tilde{w}_k^i = \frac{1}{\ell_i} \sum_{j=1}^{\ell_i} w_{\ell_i(k-1)+j}^i, \quad k = 0, \dots, N_i - 1, \quad \forall i \in \mathcal{I}_P^{\text{av}},$$

where  $\mathcal{I}_P^{\text{av}} \cup \mathcal{I}_P^{\max} \subseteq \mathcal{I}_C$ . As a result, the convolutional layer becomes  $\mathcal{C}_i = \mathcal{P}_i \circ \tilde{\mathcal{C}}_i$  in case a pooling layer is added or  $\mathcal{C}_i = \tilde{\mathcal{C}}_i$  otherwise. Finally, a CNN typically holds *fully connected* layers, which we define as mappings

$$\begin{aligned} \mathcal{L}_i: w^i &= \phi_i(W_i w^{i-1} + b_i) \quad \forall i \in \mathcal{I}_F \setminus \{l\}, \\ \mathcal{L}_l: w^l &= W_l w^{l-1} + b_l \end{aligned} \quad (3)$$

with weights  $W_i \in \mathbb{R}^{n_i \times n_{i-1}}$ , biases  $b_i \in \mathbb{R}^{n_i}$  and activation functions  $\phi_i: \mathbb{R}^{n_i} \rightarrow \mathbb{R}^{n_i}$  that are applied elementwise.

The 1D CNN  $f_\theta(w^0) = w^l$  is hence characterized by  $\theta = \{(K^i, b_i)_{i=1}^l, (W_i, b_i)_{i=p+1}^l\}$  and the chosen activation and pooling operations. In this work, we present a direct parameterization for Lipschitz-bounded 1D CNNs (1).

**Problem 1:** Find a parameterization  $\kappa \mapsto \theta$  of  $f_\theta$  for a predefined Lipschitz bound  $\rho > 0$  such that all 1D CNNs parameterized by  $\kappa$  are  $\rho$ -Lipschitz continuous with respect to the  $\ell_2$  norm, i. e., they satisfy

$$\|f_\theta(x) - f_\theta(y)\|_2 \leq \rho \|x - y\|_2 \quad \forall x, y \in \mathbb{R}^n. \quad (4)$$

In the case of multiple channels  $c$ ,  $n = cN$  denotes the stacked up version of the input. Note that  $\|\cdot\|_2$  in (4) can either be interpreted as the Euclidean norm of a vector-valued input  $x$  or as the  $\ell_2$  norm of a signal  $x$ .

To train a Lipschitz-bounded CNN, we minimize a learning objective  $\mathcal{L}(\theta)$ , e. g., the mean squared error, the cross-entropy loss or, to encourage robustness through the learning objective a tailored loss, e. g. the hinge loss [20], while at the same time enforcing Lipschitz-boundedness onto the CNN. Rather than solving a training problem subject to a Lipschitz constraint, i. e.,

$$\min_{\theta} \mathcal{L}(\theta) \quad \text{s. t.} \quad f_\theta \text{ is Lipschitz-bounded,}$$

the suggested parameterization  $\kappa \mapsto \theta$  allows to solve an unconstrained training problem over  $\kappa$

$$\min_{\kappa} \mathcal{L}(\theta(\kappa)).$$

## III. PRELIMINARIES

Before we state the parameterization of Lipschitz-bounded 1D CNNs in Section IV, we introduce a compact formulation of convolutions in state space and state LMI conditions that certify Lipschitz boundedness and that can be used to estimate the Lipschitz constant for 1D CNNs [3]. In addition, we introduce the Cayley transform used to parameterize orthogonal matrices.

### A. State space representation for convolutions

To formulate LMI conditions for convolutional layers, we can either reformulate the convolutional operation as a fully connected layer characterized by a sparse and redundant Toeplitz matrix [7] that scales with the input dimension or, as suggested in [3], we can compactly state the convolution, i. e., a finite impulse response (FIR) filter, in state space, completely independent of the input signal length. A possible discrete-time state space representation of the  $i$ -th convolutional layer (2) with state  $x_k^i \in \mathbb{R}^{n_{x_i}}$  and state dimension  $n_{x_i} = (\ell_i - 1)c_{i-1}$  is

$$\begin{aligned} x_{k+1}^i &= A_i x_k^i + B_i w_k^{i-1}, \\ y_k^i &= C_i x_k^i + D_i w_k^{i-1} + b_i, \\ w_k^i &= \phi(y_k^i), \end{aligned} \quad (5)$$

where

$$A_i = \begin{bmatrix} 0 & I & & 0 \\ 0 & 0 & \ddots & \\ \vdots & & \ddots & I \\ 0 & \dots & & 0 \end{bmatrix}, \quad B_i = \begin{bmatrix} 0 \\ \vdots \\ 0 \\ I \end{bmatrix}, \quad (6a)$$

$$C_i = [K_{\ell_{i-1}}^i \quad \dots \quad K_1^i], \quad D_i = K_0^i. \quad (6b)$$

Note that 2D convolutions also admit a state space realization, namely as a 2D system [15], based on which our parameterization can potentially be extended to end-to-end Lipschitz-bounded 2D CNNs.

**Remark 2:** The evaluation of a convolution via a fast Fourier transform necessitates the entire signal, whereas our causal representation of convolutional layers allows their use in real time.

### B. Lipschitz constant estimation

The Lipschitz constant is a sensitivity measure to changes in the input, which is commonly used to verify robustness for NNs [1]. Since, however, the calculation of the true Lipschitz constant is an NP-hard problem, an accurate upper bound is sought instead. For this purpose, we over-approximate the nonlinear activation functions by their slope-restriction cone [2], [6]. Commonly used nonlinear activation functions  $\varphi: \mathbb{R} \rightarrow \mathbb{R}$ , such as ReLU and tanh, are slope-restricted in  $[0, 1]$ , i. e.,

$$0 \leq \frac{\varphi(x) - \varphi(y)}{x - y} \leq 1 \quad \forall x, y \in \mathbb{R}^n.$$

Based on this property, we formulate an incremental quadratic constraint

$$\begin{bmatrix} \phi(x) - \phi(y) \\ x - y \end{bmatrix}^\top \begin{bmatrix} -2\Lambda & \Lambda \\ \Lambda & 0 \end{bmatrix} \begin{bmatrix} \phi(x) - \phi(y) \\ x - y \end{bmatrix} \geq 0 \quad \forall x, y \in \mathbb{R}^n. \quad (7)$$

with multipliers  $\Lambda \in \mathbb{D}_+^n$ , yielding a suitable over-approximation of the NN. The following theorem states a set of  $l$  LMI conditions that serve as a sufficient condition for Lipschitz continuity for 1D CNNs based on the relaxation (7) [3].

**Theorem 3 ([3]):** Let  $\text{CNN}_\theta$  and  $\rho > 0$  be given and let all activation functions be slope-restricted in  $[0, 1]$ . If there exist

- (i)  $Q_i \in \mathbb{S}^{c_i}$  ( $Q_i \in \mathbb{D}^{c_i}$  if a convolutional layer contains a maximum pooling layer),  $P_i \in \mathbb{S}_+^{n_{x_i}}$ , and  $\Lambda_i \in \mathbb{D}_+^{c_i}$  such that  $\forall i \in \mathcal{S}_C$

$$\left[ \begin{array}{cc|c} P_i - A_i^\top P_i A_i & -A_i^\top P_i B_i & -C_i^\top \Lambda_i \\ -B_i^\top P_i A_i & Q_{i-1} - B_i^\top P_i B_i & -D_i^\top \Lambda_i \\ \hline -\Lambda_i C_i & -\Lambda_i D_i & 2\Lambda_i - Q_i \end{array} \right] \succeq 0, \quad (8)$$

where  $Q_0 = \tilde{\rho}^2 I$ ,

- (ii)  $Q_i \in \mathbb{S}^{n_i}$  and  $\Lambda_i \in \mathbb{D}_+^{n_i}$  such that  $\forall i = \mathcal{S}_F \setminus \{l\}$

$$\begin{bmatrix} Q_{i-1} & -W_i^\top \Lambda_i \\ -\Lambda_i W_i & 2\Lambda_i - Q_i \end{bmatrix} \succeq 0 \quad \text{and} \quad \begin{bmatrix} Q_{i-1} & -W_i^\top \\ -W_i & I \end{bmatrix} \succeq 0, \quad (9)$$

where  $Q_p := I_{N_p} \otimes Q_p$ ,

then the  $\text{CNN}_\theta$  is  $\rho$ -Lipschitz continuous with  $\rho = \tilde{\rho} \prod_{s \in \mathcal{S}_P} \mu_s$ , where  $\mu_s$  are the Lipschitz constants of the average pooling layers.

The underlying idea in Theorem 3 is to enforce dissipativity onto all individual layers that are connected in a feedforward fashion. Thus the matrix  $Q_{i-1}$  links the  $i$ -th layer to the previous layer and by this interconnection we can finally analyse Lipschitz continuity of the input-output mapping  $w^l = \text{CNN}_\theta(w^0)$  [3].

Based on Theorem 3, we can determine an upper bound on the Lipschitz constant for a given CNN solving a semidefinite program

$$\min_{\rho^2, \Lambda, P, Q} \rho^2 \quad \text{s. t.} \quad (8), (9), \quad (10)$$

where  $\Lambda = \{\Lambda_i\}_{i \in \mathcal{S}_C \cup \mathcal{S}_F \setminus \{l\}}$ ,  $Q = \{Q_i\}_{i \in \mathcal{S}_C \cup \mathcal{S}_F \setminus \{l\}}$ ,  $P = \{P_i\}_{i \in \mathcal{S}_C}$  serve as decision variables together with  $\rho^2$ .

### C. Cayley transform

Typically, the Cayley transform maps skew-symmetric matrices to orthogonal matrices and its extended version parameterizes the Stiefel manifold from non-square matrices, which can be useful in designing NNs [11], [17], [21].

**Lemma 4 (Cayley transform [22]):** For all  $Y \in \mathbb{R}^{n \times n}$  and  $Z \in \mathbb{R}^{m \times n}$  the Cayley transform

$$\text{Cayley} \left( \begin{bmatrix} Y \\ Z \end{bmatrix} \right) = \begin{bmatrix} U \\ V \end{bmatrix} = \begin{bmatrix} (I+M)^{-1}(I-M) \\ 2Z(I+M)^{-1} \end{bmatrix},$$

where  $M = Y - Y^\top + Z^\top Z$ , yields matrices  $U \in \mathbb{R}^{n \times n}$  and  $V \in \mathbb{R}^{m \times n}$  that satisfy  $U^\top U + V^\top V = I$ .

Note that  $I+M$  is nonsingular since  $1 \leq \lambda_{\min}(I+Z^\top Z) \leq \text{Re}(\lambda_{\min}(I+M))$  [23].

## IV. DIRECT PARAMETERIZATION

While (10) analyses Lipschitz continuity for given 1D CNNs, it might also be desirable to train robust CNNs, i. e.,  $\rho$ -Lipschitz bounded CNNs where the robustness level  $\rho$  is chosen by the user. In this section, we introduce a direct layer-wise parameterization for 1D CNNs (1) that renders the input-output mapping Lipschitz continuous. We first discuss a parameterization for fully connected layers that satisfy (9) by design, using a similar construction to [11]. Our key contribution then is the parameterization of convolutional layers, which is carried out in two steps. In a first step, we establish a parameterization of  $P_i$  that renders the left upper block in (8) positive definite using the controllability Gramian and afterwards, we introduce the parameterization for convolutional layers that by design satisfy (8).

### A. Fully connected layers

In the following, we present a mapping  $\kappa_i \mapsto (W_i, b_i)$  from unconstrained variables  $\kappa_i$  that renders (9) feasible by design.

**Theorem 5:** Fully connected layers (3) parameterized by

$$W_i = \sqrt{2} \Gamma_i^{-1} V_i^\top L_{i-1}, \quad b_i \in \mathbb{R}^{c_i}, \quad i \in \mathcal{S}_F \setminus \{l\}, \quad (11a)$$

$$W_l = V_l^\top L_{l-1}, \quad b_l \in \mathbb{R}^{c_l}, \quad (11b)$$

satisfy (9). Herein,

$$\Gamma_i = \text{diag}(\gamma_i), L_i = \sqrt{2}U_i\Gamma_i, \begin{bmatrix} U_i \\ V_i \end{bmatrix} = \text{Cayley} \left( \begin{bmatrix} Y_i \\ Z_i \end{bmatrix} \right)$$

with free variables  $Y_i \in \mathbb{R}^{n_i \times n_i}$ ,  $Z_i \in \mathbb{R}^{n_{i-1} \times n_i}$ ,  $b_i \in \mathbb{R}^{n_i}$ ,  $i \in \mathcal{S}_F$ ,  $\gamma_i \in \mathbb{R}^{n_i}$ ,  $i \in \mathcal{S}_F \setminus \{l\}$ . This yields the mappings  $(Y_i, Z_i, \gamma_i, b_i) \mapsto (W_i, b_i)$ ,  $i \in \mathcal{S}_F \setminus \{l\}$ , and  $(Y_l, Z_l, b_l) \mapsto (W_l, b_l)$ , respectively.

*Proof:* According to Lemma 4,  $U_i$  and  $V_i$  satisfy  $U_i^\top U_i + V_i^\top V_i = I$ . Now inserting the parameterization (11a), we obtain

$$\frac{1}{2}(\Gamma_i^{-1}L_i^\top L_i\Gamma_i^{-1} + \Gamma_i W_i^\top L_{i-1}^{-1}L_{i-1}^\top W_i\Gamma_i) = I.$$

With  $Q_i = L_i^\top L_i$  and  $\Lambda_i = \Gamma_i^\top \Gamma_i$ , we further obtain

$$Q_i + \Lambda_i W_i Q_{i-1}^{-1} W_i^\top \Lambda_i = 2\Lambda_i,$$

which implies  $2\Lambda_i - Q_i - \Lambda_i W_i Q_{i-1}^{-1} W_i^\top \Lambda_i \succeq 0$ . Next, we apply the Schur complement, which yields the left inequality in (9). The last fully connected layer is a special case that does not contain an activation function. Inserting the parameterization (11b) gives

$$U_l^\top U_l + V_l^\top V_l = U_l^\top U_l + W_l Q_{l-1}^{-1} W_l^\top = I,$$

which implies  $I - W_l Q_{l-1}^{-1} W_l^\top = U_l^\top U_l \succeq 0$ , which by the application of the Schur complement satisfies the right inequality in (9). ■

Note that the connection between the auxiliary matrices  $L_i$  in (11) and  $Q_i$  in (9) is  $L_i^\top L_i = Q_i$  and the relation between the multiplier matrices  $\Lambda_i$  in (7) / (9) and  $\Gamma_i$  in (11) is  $\Gamma_i^\top \Gamma_i = \Lambda_i$ .

**Remark 6:** Throughout the paper, we assume that  $\Gamma_i$  and  $L_i$  are nonsingular. In our experiments, this was always the case. However, there also are tricks to enforce this property, e.g., by choosing  $\Gamma_i = \text{diag}(e^{\gamma_i})$  [11].

**Remark 7:** Our parameterization (11) is equivalent to the one established in [11], where they show that it is necessary and sufficient, i.e., the fully connected layers (3) satisfy (9) if and only if the weights can be parameterized by (11).

### B. Parameterization by the controllability Gramian

In this section, we make use of the controllability Gramian of (5) to parameterize convolutional layers, which to the best knowledge of the authors, has thus far not appeared in the context of parameterizing NNs. For that purpose, we introduce

$$F_i := \begin{bmatrix} P_i - A_i^\top P_i A_i & -A_i^\top P_i B_i \\ -B_i^\top P_i A_i & Q_{i-1} - B_i^\top P_i B_i \end{bmatrix} \succ 0, \quad (12)$$

which is the left upper block in (2) and further, we introduce  $\widehat{C}_i := [C_i \ D_i]$ , which simplifies the notation of (8) to

$$\begin{bmatrix} F_i & -\widehat{C}_i^\top \Lambda_i \\ -\Lambda_i \widehat{C}_i & 2\Lambda_i - Q_i \end{bmatrix} \succeq 0. \quad (13)$$

We note that the LMI (13) and the left LMI in (9) share a similar structure. The right lower block is the same in both LMIs. In addition to the bias terms  $b_i$ , the parameters to be trained in the CNN layers are collected in  $\widehat{C}_i$ , cmp. (6),

whereas the parameters  $W_i$  characterize the fully connected layers. In the off-diagonal blocks of the respective LMIs (13) and (9)  $\widehat{C}_i$  and  $W_i$  appear respectively multiplied by  $\Lambda_i$ . The only difference is in the left upper blocks of the LMIs. While in LMI (9) for fully connected layers, we here have  $Q_{i-1} = L_{i-1}^\top L_{i-1} \succ 0$  for nonsingular  $L_{i-1}$ , LMI (13) for convolutional layers here contains  $F_i$ , that depends on  $Q_{i-1}$ . To render  $F_i$  positive definite, we parameterize  $P_i$  as follows, using the controllability Gramian.

**Lemma 8:** For some  $\varepsilon > 0$  and all  $H_i \in \mathbb{R}^{n_{x_i} \times n_{x_i}}$ , the matrix  $P_i = X_i^{-1}$  with

$$X_i = \sum_{k=0}^{n_{x_i} - c_{i-1}} A_i^k (B_i Q_{i-1}^{-1} B_i^\top + H_i^\top H_i + \varepsilon I) (A_i^\top)^k, \quad (14)$$

renders (12) feasible.

*Proof:* The matrix  $A_i$  is a nilpotent matrix, i.e.,  $A_i^{n_{x_i} - c_{i-1} + k} = 0 \ \forall k \geq 1$ , such that

$$X_i = \sum_{k=0}^{\infty} A_i^k (B_i Q_{i-1}^{-1} B_i^\top + H_i^\top H_i + \varepsilon I) (A_i^\top)^k$$

corresponds to the controllability Gramian of the linear time-invariant system characterized by  $(A_i, B_i)$  as defined in (6a), i.e., the unique solution  $X_i \succ 0$  to the Lyapunov equation

$$X_i - A_i X_i A_i^\top - B_i Q_{i-1}^{-1} B_i^\top = H_i^\top H_i + \varepsilon I \succ 0. \quad (15)$$

Note that  $X_i$  is positive definite by design, given that  $Q_{i-1} = L_{i-1}^\top L_{i-1} \succ 0$  such that  $B_i Q_{i-1}^{-1} B_i^\top + H_i^\top H_i + \varepsilon I$  is positive definite. Next, we apply the Schur complement to (15) to obtain

$$\begin{bmatrix} X_i^{-1} & 0 & A_i^\top \\ 0 & Q_{i-1} & B_i^\top \\ A_i & B_i & X_i \end{bmatrix} \succ 0,$$

Now inserting  $P_i = X_i^{-1}$  and again applying the Schur complement yields (12). ■

### C. Convolutional layers

In this subsection, we present a direct parameterization for convolutional layers such that they satisfy (13) by design. Our parameterization of convolution kernels  $K^i \in \mathbb{R}^{c_i \times c_{i-1} \times \ell_i}$ , or equivalently  $\widehat{C}_i \in \mathbb{R}^{c_i \times \ell_i c_{i-1}}$ , is independent of the input dimension  $N_i$  whereas other approaches design a parameterization for Lipschitz-bounded convolutions and CNNs in the Fourier domain which involves the costly inversion of  $N_i$  matrices [17], [11].

**Theorem 9:** Convolutional layers (2) that contain an average pooling layer or no pooling layer parameterized by

$$\widehat{C}_i = \sqrt{2} \Gamma_i^{-1} V_i^\top L_i^F, \quad b_i \in \mathbb{R}^{c_i}, \quad \forall i \in \mathcal{S}_C \setminus \mathcal{S}_C^{\max} \quad (16)$$

satisfy (8). Herein,

$$\Gamma_i = \text{diag}(\gamma_i), \quad \begin{bmatrix} U_i \\ V_i \end{bmatrix} = \text{Cayley} \left( \begin{bmatrix} Y_i \\ Z_i \end{bmatrix} \right), \quad L_i^F = \text{chol}(F_i),$$

$\text{chol}(\cdot)$  denoting the Cholesky decomposition,  $Q_i = L_i^\top L_i$ ,  $L_0 = \rho I$ ,  $L_i = \sqrt{2}U_i\Gamma_i$ , where  $F_i$  is given by (12) with  $P_i$  parameterized from  $Q_{i-1}$  and  $H_i$  using (14). The free variables beside  $b_i$  are  $Y_i \in \mathbb{R}^{c_i \times c_i}$ ,  $Z_i \in \mathbb{R}^{\ell_i c_{i-1} \times c_i}$ ,  $H_i \in$

$\mathbb{R}^{n_{x_i} \times n_{x_i}}$ ,  $\gamma_i \in \mathbb{R}^{c_i}$ ,  $i \in \mathcal{S}_C \setminus \mathcal{S}_C^{\max}$ , which yields the mapping  $(Y_i, Z_i, H_i, \gamma_i, b_i) \mapsto (K^i, b_i)$ .

*Proof:* The matrices  $U_i$  and  $V_i$  satisfy  $U_i^\top U_i + V_i^\top V_i = I$ . Now inserting the parameterization (16), we obtain

$$\frac{1}{2}(\Gamma_i^{-1} L_i^\top L_i \Gamma_i^{-1} + \Gamma_i W_i^\top L_{i-1}^{F_i} L_{i-1}^{F_i}{}^{-\top} W_i \Gamma_i) = I.$$

Lemma 8 ensures positive definiteness of  $F_i$ , i.e., its Cholesky decomposition exists, and we insert  $Q_i = L_i^\top L_i$ ,  $F_i = L_i^{F_i} L_i^{F_i}$ ,  $\Lambda_i = \Gamma_i^\top \Gamma_i$ , to further obtain

$$Q_i + \Lambda_i \widehat{C}_i F_i^{-1} \widehat{C}_i^\top \Lambda_i = 2\Lambda_i,$$

which implies  $2\Lambda_i - Q_i - \Lambda_i \widehat{C}_i F_i^{-1} \widehat{C}_i^\top \Lambda_i \succeq 0$ . Next, we apply the Schur complement and obtain (13) which corresponds to (8). ■

To account for average pooling layers present in the CNN, we rescale the Lipschitz bound with the product of the Lipschitz bounds of the average pooling layers, i.e.,  $\tilde{\rho} = \rho / \prod_{s \in \mathcal{S}_p^{\text{av}}} \text{cmp}$ . Theorem 3, and then we use (16) to parameterize the convolutional layer.

#### D. Maximum pooling layers

In case there is a maximum pooling layer in  $\mathcal{C}_i$ , i.e.  $\mathcal{C}_i = \mathcal{P}_i^{\max} \circ \mathcal{C}_i$ , we need to parameterize  $Q_i$  as a diagonal matrix, cmp. Theorem 3, which also affects the parameterization. This constraint comes from the incremental quadratic constraint used to include maximum pooling layers [3]. While average pooling is a linear operation and allows for full matrices  $Q_i$ , the nonlinearity of the maximum pooling layer is the reason for the additional diagonality constraint.

**Corollary 10:** Convolutional layers (3) that contain a maximum pooling layer parameterized by

$$\widehat{C}_i = \Lambda_i^{-1} \tilde{\Gamma}_i \tilde{U}_i^\top L_i^{F_i}, \quad b_i \in \mathbb{R}^{c_i}, \quad \forall \mathcal{S}_C^{\max} \quad (17)$$

satisfy (8). Herein,

$$\Lambda_i = \frac{1}{2} \left( \tilde{\Gamma}_i^\top \tilde{\Gamma}_i + Q_i \right), \quad \tilde{\Gamma}_i = \text{diag}(\tilde{\gamma}_i), \quad \tilde{U}_i = \text{Cayley}(\tilde{Y}_i),$$

$Q_i = L_i^\top L_i$ ,  $L_0 = \rho I$ ,  $L_i = \text{diag}(l_i)$ ,  $L_i^{F_i} = \text{chol}(F_i)$ , where  $F_i$  is given by (12) with  $P_i$  parameterized from  $Q_{i-1}$  and  $H_i$  using (14). The free variables  $\tilde{Y}_i \in \mathbb{R}^{l_i c_{i-1} \times c_i}$ ,  $H_i \in \mathbb{R}^{n_{x_i} \times n_{x_i}}$ ,  $\tilde{\gamma}_i, l_i \in \mathbb{R}^{c_i}$ ,  $i \in \mathcal{S}_C^{\max}$  compose the mapping  $(\tilde{Y}_i, H_i, \tilde{\gamma}_i, l_i, b_i) \mapsto (K^i, b_i)$ .

*Proof:* Using that  $\tilde{U}_i$  satisfies  $\tilde{U}_i^\top \tilde{U}_i = I$ , we insert (17) and we replace  $F_i = L_i^{F_i} L_i^{F_i}$ , whose Cholesky decomposition exists by Lemma 8, to obtain

$$\Lambda_i \widehat{C}_i F_i^{-1} \widehat{C}_i^\top \Lambda_i = \tilde{\Gamma}_i^\top \tilde{\Gamma}_i = 2\Lambda_i - Q_i,$$

which implies  $2\Lambda_i - Q_i - \Lambda_i \widehat{C}_i F_i^{-1} \widehat{C}_i^\top \Lambda_i \succeq 0$ , which by the application of the Schur complement satisfies (13). ■

#### E. $\rho$ -Lipschitz layers

In this work, we enforce Lipschitz continuity onto the input-output mapping of the CNN, which is more general and less conservative than approaches that include Lipschitz guarantees for the individual layers, using that the product of

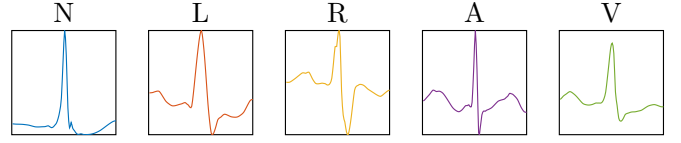


Fig. 1: Different heart wave classes.

the Lipschitz bounds gives the Lipschitz bound for the NN [18].

**Corollary 11:** The  $i$ -th linear fully connected layer

$$v^i = W_i w^{i-1} + b_i \quad \text{with} \quad W_i = \rho \tilde{U}_i^\top, \quad b_i \in \mathbb{R}^{n_i},$$

is  $\rho$ -Lipschitz continuous, where  $\tilde{U}_i = \text{Cayley}(\tilde{Y}_i)$ , and  $\tilde{Y}_i \in \mathbb{R}^{n_{i-1} \times n_i}$  is a free variable, which yields the mapping  $(\tilde{Y}_i, b_i) \mapsto (W_i, b_i)$ .

**Corollary 12:** The  $i$ -th 1D convolution

$$v_i = b_i + \sum_{j=0}^{\ell_i-1} K_j^i w_{k-j}^{i-1} \quad \text{with} \quad \widehat{C}_i = \tilde{U}_i^\top L_i^{F_i}, \quad b_i \in \mathbb{R}^{c_i},$$

where  $K^i$  is recovered according to (6b), is  $\rho$ -Lipschitz continuous. Herein,  $\tilde{U}_i = \text{Cayley}(\tilde{Y}_i)$ ,  $L_i^{F_i} = \text{chol}(F_i)$ , where  $F_i$  is given by (12) with  $P_i$  parameterized from  $Q_{i-1} = \rho^2 I$  and  $H_i$  using (14). Beside  $b_i$  the free variables are  $\tilde{Y}_i \in \mathbb{R}^{l_i c_{i-1} \times c_i}$ ,  $H_i \in \mathbb{R}^{n_{x_i} \times n_{x_i}}$ , yielding the mapping  $(\tilde{Y}_i, H_i, b_i) \mapsto (K^i, b_i)$ .

The proofs of Corollaries 11 and 12 follow along the lines of the proof of Corollary 10.

## V. SIMULATION RESULTS

In this section, we train Lipschitz-bounded 1D CNNs (LipCNNs) to classify heart arrhythmia data from the MIT-BIH database, an ECG database [19], in its preprocessed form [24] that assigns heart wave signals to one of the five classes depicted in Fig. 1: N (normal beat), L (left bundle branch block), R (right bundle branch block), A (atrial premature contraction), V (ventricular premature contraction). In particular, we use 26,490 samples, 13,245 training data points and 13,245 test data points. Fig. 2a shows the architecture of the 1D CNN used to train on the ECG dataset, where we chose the cross-entropy loss as the training objective. For training, we use Flux and JuMP in Julia in combination with MOSEK [25] on a standard i7 notebook<sup>1</sup>.

We compare our approach to vanilla CNNs, and L2 regularized CNNs with different weighting factors  $\gamma$ . To evaluate the robustness of the CNNs, we compute the test accuracy on adversarial examples from the L2 projected gradient descent attack for different perturbation strengths, which is shown in Fig. 2b. Note that the two shown LipCNNs indicate comparably high test accuracies to the shown vanilla and L2 regularized CNNs on unperturbed data while maintaining higher accuracies than their counterparts as the perturbation strength increases. Further, Table I shows the averaged test accuracies and upper and lower Lipschitz bounds for different 1D CNNs and Fig. 3 illustrates the tradeoff between accuracy and robustness. For low Lipschitz bounds we observe high

<sup>1</sup>Code is available at [www.github.com/ppauli/1D-LipCNNs](http://www.github.com/ppauli/1D-LipCNNs).

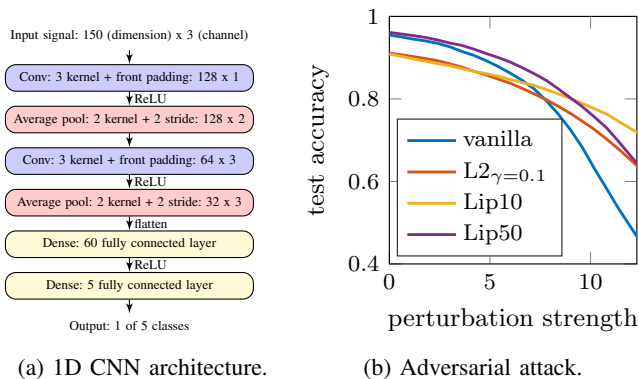


Fig. 2: (a) CNN used for ECG dataset. (b) Vanilla, L2 regularized ( $\gamma = 0.1$ ) and Lipschitz ( $\rho = 50$ ) CNN on adversarial examples with different perturbation strengths  $\epsilon$  created using the L2 projected gradient descent attack [26].

TABLE I: Test accuracy and Lipschitz upper bound [3] and empirical Lipschitz lower bound of trained CNNs, averaged over 5 CNNs.

	vanilla	L2 $\gamma=0.05$	L2 $\gamma=0.1$	Lip5	Lip10	Lip50
Test acc.	94.9%	92.4%	90.6%	84.8%	90.0%	94.7%
Lip. UB	147	45.7	33.9	4.99	9.85	45.3
Emp. LB	28.3	13.2	10.2	2.20	4.06	15.1

robustness, yet lower test accuracies and vice versa. We note that the vanilla CNN has significantly larger upper Lipschitz bounds than LipCNN and further, LipCNN maintains high test accuracies as the Lipschitz bound decreases in Fig. 3. With even larger weighting parameters  $\gamma$  in L2 regularized training the training failed, whereas LipCNNs allows for training with very low Lipschitz bounds.

## VI. CONCLUSION

In this paper, we introduced a parameterization for Lipschitz-bounded 1D CNNs using Cayley transforms and controllability Gramians. Using our parameterization we can train Lipschitz-bounded 1D CNNs in an unconstrained training problem which we illustrated in the classification of ECG data from the MIT-BIH database. Future research includes the extension of our parameterization to 2D CNNs using a 2D systems approach as suggested in [15].

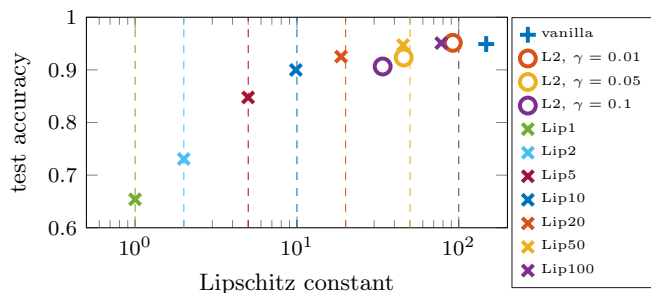


Fig. 3: Accuracy robustness tradeoff. Test accuracy over Lipschitz constant from SDP [3], averaged over 5 CNNs.

## REFERENCES

- [1] C. Szegedy, W. Zaremba, I. Sutskever, J. Bruna, D. Erhan, I. Goodfellow, and R. Fergus, "Intriguing properties of neural networks," *arXiv preprint arXiv:1312.6199*, 2013.
- [2] M. Fazlyab, A. Robey, H. Hassani, M. Morari, and G. Pappas, "Efficient and accurate estimation of Lipschitz constants for deep neural networks," *Advances in Neural Information Processing Systems*, vol. 32, 2019.
- [3] P. Pauli, D. Gramlich, and F. Allgöwer, "Lipschitz constant estimation for 1D convolutional neural networks," *arXiv preprint arXiv:2211.15253*, 2022.
- [4] P. L. Combettes and J.-C. Pesquet, "Deep neural network structures solving variational inequalities," *Set-Valued and Variational Analysis*, vol. 28, no. 3, pp. 491–518, 2020.
- [5] F. Latorre, P. Rolland, and V. Cevher, "Lipschitz constant estimation of neural networks via sparse polynomial optimization," *arXiv preprint arXiv:2004.08688*, 2020.
- [6] P. Pauli, A. Koch, J. Berberich, P. Kohler, and F. Allgöwer, "Training robust neural networks using Lipschitz bounds," *IEEE Control Systems Letters*, vol. 6, pp. 121–126, 2022.
- [7] P. Pauli, N. Funcke, D. Gramlich, M. A. Msalmi, and F. Allgöwer, "Neural network training under semidefinite constraints," *arXiv preprint arXiv:2201.00632*, 2022.
- [8] H. Gouk, E. Frank, B. Pfahringer, and M. J. Cree, "Regularisation of neural networks by enforcing Lipschitz continuity," *Machine Learning*, vol. 110, no. 2, pp. 393–416, 2021.
- [9] M. Revay, R. Wang, and I. R. Manchester, "Lipschitz bounded equilibrium networks," *arXiv preprint arXiv:2010.01732*, 2020.
- [10] —, "Recurrent equilibrium networks: Flexible dynamic models with guaranteed stability and robustness," *arXiv preprint arXiv:2104.05942*, 2021.
- [11] R. Wang and I. R. Manchester, "Direct parameterization of Lipschitz-bounded deep networks," *arXiv preprint arXiv:2301.11526*, 2023.
- [12] J. Gu, Z. Wang, J. Kuen, L. Ma, A. Shahroudy, B. Shuai, T. Liu, X. Wang, G. Wang, J. Cai *et al.*, "Recent advances in convolutional neural networks," *Pattern recognition*, vol. 77, pp. 354–377, 2018.
- [13] S. Kiranyaz, O. Avci, O. Abdeljaber, T. Ince, M. Gabbouj, and D. J. Inman, "1D convolutional neural networks and applications: A survey," *Mechanical systems and signal processing*, vol. 151, p. 107398, 2021.
- [14] A. v. d. Oord, S. Dieleman, H. Zen, K. Simonyan, O. Vinyals, A. Graves, N. Kalchbrenner, A. Senior, and K. Kavukcuoglu, "Wavenet: A generative model for raw audio," *arXiv preprint arXiv:1609.03499*, 2016.
- [15] D. Gramlich, P. Pauli, C. W. Scherer, F. Allgöwer, and C. Ebenbauer, "Convolutional neural networks as 2-D systems," *arXiv preprint arXiv:2303.03042*, 2023.
- [16] C. Anil, J. Lucas, and R. Grosse, "Sorting out lipschitz function approximation," in *International Conference on Machine Learning*. PMLR, 2019, pp. 291–301.
- [17] A. Trockman and J. Z. Kolter, "Orthogonalizing convolutional layers with the Cayley transform," *arXiv preprint arXiv:2104.07167*, 2021.
- [18] A. Araujo, A. J. Havens, B. Delattre, A. Allauzen, and B. Hu, "A unified algebraic perspective on lipschitz neural networks," in *11th International Conference on Learning Representations*, 2023.
- [19] <http://www.physionet.org/physiobank/database/mitdb/>.
- [20] L. Béthune, T. Boissin, M. Serrurier, F. Mamalet, C. Friedrich, and A. González-Sanz, "Pay attention to your loss: understanding misconceptions about 1-lipschitz neural networks," *arXiv preprint arXiv:2104.05097*, 2021.
- [21] K. Helfrich, D. Willmott, and Q. Ye, "Orthogonal recurrent neural networks with scaled Cayley transform," in *International Conference on Machine Learning*. PMLR, 2018, pp. 1969–1978.
- [22] M. Jauch, P. D. Hoff, and D. B. Dunson, "Random orthogonal matrices and the Cayley transform," *Bernoulli*, vol. 26, no. 2, pp. 1560–1586, 2020.
- [23] E. De Klerk, *Aspects of semidefinite programming: interior point algorithms and selected applications*. Springer Science & Business Media, 2006, vol. 65.
- [24] S. Abuadba, "split-learning-1d," <https://github.com/SharifAbuadba/split-learning-1d>, 2020.
- [25] M. ApS, *The MOSEK optimization toolbox. Version 10.0.*, 2022. [Online]. Available: <http://docs.mosek.com/10.0/toolbox/index.html>
- [26] A. Madry, A. Makelov, L. Schmidt, D. Tsipras, and A. Vladu, "Towards deep learning models resistant to adversarial attacks," *arXiv preprint arXiv:1706.06083*, 2017.